Another Way of Looking at Plane-Based Calibration: the Centre Circle Constraint

Pierre Gurdjos, Alain Crouzil and René Payrissat

IRIT-TCI, Université Paul Sabatier,
118, route de Narbonne
31062 Toulouse Cedex 4, FRANCE
gurdjos@irit.fr crouzil@irit.fr payrissa@irit.fr

Abstract. The plane-based calibration consists in recovering the internal parameters of the camera from the views of a planar pattern with a known geometric structure. The existing direct algorithms use a problem formulation based on the properties of basis vectors. They minimize algebraic distances and may require a 'good' choice of system normalization. Our contribution is to put this problem into a more intuitive geometric framework. A solution can be obtained by intersecting circles, called Centre Circles, whose parameters are computed from the world-to-image homographies. The Centre Circle is the camera centre locus when planar figures are in perpective correspondence, in accordance with a Poncelet's theorem. An interesting aspect of our formulation, using the Centre Circle constraint, is that we can easily transform the cost function into a sum of squared Euclidean distances. The simulations on synthetic data and an application with real images confirm the strong points of our method.
Keywords. Calibration, Homography, Planar Scene, Multiple View Geometry, Poncelet.

1 Introduction

The metric information of the camera is partially encoded through a set of parameters, called internal parameters of the camera. The 'plane-based calibration' problem consists in recovering the internal parameters of the camera from n different views of a planar object lying on some reference plane Π, providing that Euclidean information about Π is available (*e.g.* coordinate system, angle, length ratio, etc.). If no Euclidean structure of the plane is available, this problem then refers to 'autocalibration from planes' [13][8]. Apart from the fact that, in many man-made environments, planes are widely present and easily identifiable, an important advantage of plane-based autocalibration [4, § 18.7, pp. 470-471] is that it only requires to know the homography matrices induced by world planes, whose estimations are much stable and accurate than those of inter-image transformations arising from projections of 3D points, *e.g.* the fundamental matrix. Once the internal parameters are recovered, the estimation of the relative pose between planes and cameras (*i.e.* the external parameters of the camera) can be achieved [12].

The issue of plane-based calibration has been widely studied during the past years [2][9][8][11][14]. Fundamentally, as for the problem formulation, one very determining result has been to highlight some imaginary projective entities, in particular the absolute conic [1, § 2.5.8, pp. 29-30], whose image encodes the Euclidean information related to the camera. This enables to define a generic framework for calibration based on the properties of basis vector in Π [13]. In particular, each world-to-image homography, induced by Π, yields two constraints, that basically represent the orthogonality and the equality of norms of the imaged basis vectors, with respect to the imaged absolute conic. Using these constraints, the plane-based calibration problem consists in estimating the parameter matrix of the imaged absolute conic [14][11][7][4]. Fortunately, the two constraints can be linearized and the problem can therefore can be solved using direct (*i.e.* non-iterative) least-squares techniques. As the relation between the internal parameters of the camera and the elements of the parameter matrix of the imaged absolute conic is one-to-one, one can estimate the former set of parameters by estimating the latter. These algorithms are easy to implement and fast. They also proved to be efficient, providing that there are no critical camera displacements [11]. However, in search of a 'better' estimation, one may criticize the existing algorithms for minimizing algebraic error functions. It follows that it is not straightforward to explicit what is actually minimized during the estimation process. Moreover, in certain cases, a good choice of 'system normalization' can be required to obtain reliable results.

Our contribution is to put the plane-based calibration problem into a more intuitive geometric framework, in accordance with a theorem of J.V. Poncelet. In the middle of the XIX^e century, Poncelet stated some geometric properties deduced from two planar figures in perspective correspondence and, in particular, about the positions of the centres of projection. We show that the solution of the plane-based calibration problem can be obtained by intersecting circles (called *Centre Circles*) whose parameters can be easily computed from the world-to-image homographies. For one view, the Centre Circle is the locus of the camera centre (*i.e.* the set of multiple solutions). To put it more precisely, the Centre Circle equation can be represented by two equations, the former defining a plane (called *Centre Plane*) and the latter a sphere (called *Centre Sphere*). We show that these two equations and the two equations based on the properties of basis vectors are equivalent. Nevertheless, we exhibit two interesting aspects of our formulation. The first aspect is that we can easily transform (in most cases) the algebraic error functions into a sum of squared Euclidean distances. The second aspect is that the Centre Plane equation is irrespective of the focal length. This latter property makes it possible for us to describe a two-step method for calibrating a camera with varying focal length. At first, the constant parameters are estimated, then the m different focal lengths are directly computed from each 'partially calibrated' view. It is worthy of note that the complexity of our algorithm is in $\mathcal{O}(m)$ while it was in $\mathcal{O}(m^3)$ in the existing methods.

Notations. A scalar is denoted by a non-bold letter X, u or ω. A vector is denoted by a lowercase bold letter, *e.g.* $\mathbf{x}$. A matrix is denoted by an uppercase

bold letter, *e.g.* $\mathbf{M}$, or a Greek bold letter, *e.g.* $\boldsymbol{\omega}$. We use $\mathrm{diag}(d_1, \cdots, d_n)$ for denoting the diagonal (square) matrix of order n with the elements $d_1, \cdots, d_n$ on the main diagonal. The column vectors of matrix $\mathbf{M}$ are denoted by $\mathbf{m}_j$ and its elements are denoted by M_{ij}. We use the Matlab-like notation $\mathbf{M}_{(1:r,1:c)}$ for denoting the $r \times c$ submatrix of $\mathbf{M}$ selected by the row range $1 : r$ and the column range $1 : c$. The notation $\mathbf{M}_{(:,1:c)}$ (resp. $\mathbf{M}_{(1:r,:)}$), selects the first c (resp. r) columns (resp. rows) of $\mathbf{M}$. A set of n objects, *e.g.* n matrices $\mathbf{M}$, is denoted by $\mathbf{M}^{(1)}, \mathbf{M}^{(2)} \ldots \mathbf{M}^{(n)}$. Notation $\mathbf{x} \sim \mathbf{y}$ means that $\mathbf{x}$ is equal to $\mathbf{y}$, up to a scalar factor.

2 Outline of Existing Plane-Based Calibration Methods

2.1 Plane-Based Calibration Equations

The Euclidean world coordinates (X, Y, Z) of a point and its imaged pixel coordinates (u, v) are related by the projection equation $[u, v, 1]^\top \sim \mathbf{P}[X, Y, Z, 1]^\top$. The 3×4 perspective projection matrix $\mathbf{P}$ can be decomposed as $\mathbf{P} = \mathbf{A}[\mathbf{R} \mid \mathbf{t}]$, where $\mathbf{A}$ is the calibration matrix and $(\mathbf{R}, \mathbf{t})$ describes the object with respect to the camera coordinate system. The matrix $\mathbf{A}$ is the upper triangular matrix, given in (1), that encodes the internal parameters of the camera: f is the focal length (in pixels) with respect to the u-axis, τ is the aspect ratio parameter (unit-less) and (u_0, v_0) are the pixel coordinates of the principal point. We assume that the object is planar, lying on the world plane $\mathit{\Pi}$ with equation $Z = 0$ with respect to the world coordinate system. Consequently, the world-to-image homography matrix $\mathbf{H}$, describing the restriction of $\mathbf{P}$ to $\mathit{\Pi}$, admits the following decomposition

$$\mathbf{H} = \mathbf{A} \begin{bmatrix} \mathbf{r}_1 & \mathbf{r}_2 & \mathbf{t} \end{bmatrix}, \quad \text{where } \mathbf{A} = \begin{bmatrix} f & 0 & u_0 \\ 0 & -\tau f & v_0 \\ 0 & 0 & 1 \end{bmatrix}. \tag{1}$$

The vector $\mathbf{r}_i$ denotes the ith column of the rotation matrix $\mathbf{R}$. Considering $\mathbf{r}_1, \mathbf{r}_2$ as basis vectors in $\mathit{\Pi}$, the properties $\mathbf{r}_1^\top \mathbf{r}_2 = 0$ and $\|\mathbf{r}_1\|^2 = \|\mathbf{r}_2\|^2$ transform under $\mathbf{P}$ into

$$\mathbf{h}_1^\top \boldsymbol{\omega} \mathbf{h}_2 = 0, \quad \mathbf{h}_1^\top \boldsymbol{\omega} \mathbf{h}_1 = \mathbf{h}_2^\top \boldsymbol{\omega} \mathbf{h}_2, \tag{2}$$

where $\mathbf{h}_1$et $\mathbf{h}_2$ are the first two columns of $\mathbf{H}$; the matrix $\boldsymbol{\omega}$ represents the image of the absolute conic [1] such that

$$\boldsymbol{\omega} = \begin{bmatrix} \tau^2 & 0 & -\tau^2 u_0 \\ 0 & 1 & -v_0 \\ -\tau^2 u_0 & -v_0 & \tau^2 u_0^2 + v_0^2 + \tau^2 f^2 \end{bmatrix} \sim \mathbf{A}^{-\top} \mathbf{A}^{-1}. \tag{3}$$

As for camera self-constraints, it is known [4] that the following equalities hold

$$\omega_{12} = 0, \qquad \omega_{11} = \tau^2 \omega_{22}, \tag{4}$$

$$u_0 \omega_{11} = -\omega_{13}, \qquad v_0 \omega_{22} = -\omega_{23}. \tag{5}$$

2.2 Linearization of the Plane-Based Calibration Equations

A. Constant internal parameters. A single world-to-image homography matrix $\mathbf{H}$ yields 2 constraints (2) on the 5 elements of symmetric matrix $\boldsymbol{\omega}$. If we represent these 5 unknowns by $\mathbf{x} \sim [\omega_{13}, \omega_{23}, \omega_{11}, \omega_{22}, \omega_{33}]^\top$, then the constraints (2) can be linearized as the 2 homogeneous equations $\left[\, \mathbf{a} \mid \mathbf{b} \,\right]^\top \mathbf{x} = 0$, where

$$\begin{array}{l} \mathbf{a} = \left[\begin{array}{ccccc} H_{11}H_{32}+H_{12}H_{31}, & H_{22}H_{31}+H_{21}H_{32}, & H_{11}H_{12}, & H_{21}H_{22}, & H_{31}H_{32} \end{array} \right]^\top, \\ \mathbf{b} = \left[\begin{array}{cccc} 2(H_{11}H_{31}-H_{12}H_{32}), & 2(H_{21}H_{31}-H_{22}H_{32}), & H_{11}^2-H_{12}^2, & H_{21}^2-H_{22}^2, \; H_{31}^2-H_{32}^2 \end{array} \right]^\top. \end{array} \quad (6)$$

By enforcing the additional constraint $\|\mathbf{x}\| = 1$, at least 2 images are required to obtain a solution.

B. Varying focal length. When the focal length f varies, its different values can be considered as additional unknowns. Indeed, in (3), all the elements are irrespective of f, except ω_{33}. We distinguish between the different ω_{33} by using the notation $\omega_{33}^{(j)}$ $(1 \leq j \leq m)$, where m is the number of different focal lengths. Accordingly, the $(4 + m)$ unknowns can be represented by $\mathbf{x} \sim [\omega_{13}, \omega_{23}, \omega_{11}, \omega_{22}, \omega_{33}^{(1)}, \ldots, \omega_{33}^{(m)}]^\top$. The matrix $\left[\, \mathbf{a} \mid \mathbf{b} \,\right]^\top$ is now a $2\times(4+m)$ matrix defined as:

$$\mathbf{a} = \left[a_1, a_2, a_3, a_4, \mathbf{0}_{j-1}^\top, a_5, \mathbf{0}_{m-j}^\top\right]^\top, \quad \mathbf{b} = \left[b_1, b_2, b_3, b_4, \mathbf{0}_{j-1}^\top, b_5, \mathbf{0}_{m-j}^\top\right]^\top, \quad (7)$$

where a_i (resp. b_i) is the ith element of $\mathbf{a}$ (resp. $\mathbf{b}$) given in (6). By enforcing $\|\mathbf{x}\| = 1$, at least 4 images are required to obtain a solution.

Algorithm. The procedure is as follows. Given n homography matrices:

1. Stack the $2n$ row vectors $\mathbf{a}^\top, \mathbf{b}^\top$ as given in (6) or (7) into a matrix $\mathbf{F}$.
2. Find
$$\hat{\mathbf{x}} = \mathbf{W}_R \arg\min_{\mathbf{x}} (\|\mathbf{W}_L \mathbf{F} \mathbf{W}_R \mathbf{x}\|^2), \quad \text{subject to } \|\mathbf{x}\| = 1,$$
given the adequate metric in terms of left-hand and right-hand weighting matrices $\mathbf{W}_L$, $\mathbf{W}_R$.
3. Recover the internal parameters from (4) and (5).

Such a *Total Least-Squares (TLS)* solution [5] can be obtained by means of a singular value decomposition (SVD) of the $2n\times(4+m)$ matrix $\mathbf{F}$, where m is the number of the different focal lengths. The elements of $\mathbf{F}$ may differ in magnitude in a very sizeable way. This may lead to a bad system conditioning that a right-hand equilibration of $\mathbf{F}$ (*e.g.* a column scaling such as to have equal norms as suggested in [11]) can highly improve. It is worthy of note that equilibrating may be very determining, in particular with regard to the case 2.2.B.

This approach has been utilized by Z. Zhang [14], with regard to 2.2.A, and P. Sturm & S. Maybank [11], with regard to 2.2.B. Although a geometric interpretation of basic equations (2) is given in [14], within a projective framework, it is not straightforward to explicit what is actually minimized. This is notably owing to the fact that the homography matrices are only known up to a scale

factor that varies with each image. This is why we claim that the cost functions used in the algorithm described in 2.2 are based on algebraic distances. As a general rule, it is known that algebraic error functions are not geometrically or statistically meaningful and the obtained solutions may not be those expected intuitively [4]. On the other hand, computing the solution may require a SVD decomposition that can be extensive, regarding the algorithm complexity. As shown in [2], the required amount of flops is in $\mathcal{O}(m^3)$. With regard to real time-like calibration, we assert that, providing that the estimator is consistent, *i.e.* converges to the true value as n tends to infinity, the minimization algorithm must exhibit a low complexity, *i.e.* in $\mathcal{O}(m)$.

3 A Centre Circle approach to Plane-Based Calibration

The primary motivation of this paper is to seek a direct method that does not reveal the disadvantages discussed in the previous section. In this section, we first consider the transformation of the basic equations. Such a normalization step turns out to be quite interesting because it enables us to connect the plane-base calibration problem to a Poncelet's theorem. This theorem is then discussed, as for its importance in selecting a 'good' minimization criterion.

3.1 Transformation of the Basic Equations

The coordinates of points in plane Π are usually given with an origin arbitrarily chosen. It can readily be seen that any homography of the form $\mathbf{HS}$, where $\mathbf{S}$ is a matrix representing a similarity of the projective plane, also satisfies the basic constraints (2). The fact of post-multiplying $\mathbf{H}$ by $\mathbf{S}$ amounts to apply a change of coordinates in plane Π. Consider the similarity matrix $\mathbf{S} = \left[\bar{\mathbf{i}}\ \bar{\mathbf{j}}\ \bar{\mathbf{k}}\right]$, whose columns are $\bar{\mathbf{i}} = \frac{1}{n}\left[H_{31}, H_{32}, 0\right]^\top$, $\bar{\mathbf{j}} = \frac{1}{n}\left[-H_{32}, H_{31}, 0\right]^\top$ and $\bar{\mathbf{k}} = [0, 0, 1]^\top$, where n is a scale factor [1]. The transformed homography matrix is given by

$$\bar{\mathbf{H}} = \mathbf{HS} = \begin{bmatrix} \frac{1}{n}(H_{11}H_{31} + H_{12}H_{32}) & \frac{1}{n}(H_{12}H_{31} - H_{11}H_{32}) & H_{13} \\ \frac{1}{n}(H_{21}H_{31} + H_{22}H_{32}) & \frac{1}{n}(H_{22}H_{31} - H_{21}H_{32}) & H_{23} \\ n & 0 & H_{33} \end{bmatrix}. \quad (8)$$

It is easy to see that (8) is equivalent to $\bar{\mathbf{h}} = \mathbf{Dh}$, where $\bar{\mathbf{h}}$ (resp. $\mathbf{h}$) denotes the 3×2 submatrix $\bar{\mathbf{H}}_{(:,1:2)}$ (resp. $\mathbf{H}_{(:,1:2)}$) as a single 6×1 vector obtained by stacking the elements in order 'row-first' and $\mathbf{D} = \mathrm{diag}(\bar{\mathbf{S}}^\top, \bar{\mathbf{S}}^\top, \bar{\mathbf{S}}^\top)$ is a 6×6 matrix [2] ; $\bar{\mathbf{S}}$ denoting the 2×2 submatrix $\mathbf{S}_{(1:2,1:2)}$. As a result, $\bar{H}_{32} = 0$ always holds, whatever the camera orientation. From a geometrical point of view, this means that the vanishing point associated with one basis vector of Π

[1] We suggest $n = \sqrt{H_{31}^2 + H_{32}^2}$ ($\mathbf{S}$ is then a rotation matrix) although the only justification we can give in this paper for such a choice is empirical.

[2] Notation-wise, $\mathrm{diag}(\cdot)$ is here generalized to block matrices.

is *always* at infinity or, equivalently, that this basis vector is *always* parallel to the intersection line of Π with the image plane.

Accordingly, substituting $\bar{\mathbf{h}}$ for $\mathbf{h}$ in (2), the basic equations are then linearized as $\left[\,\bar{\mathbf{a}} \mid \bar{\mathbf{b}}\,\right]^\top \mathbf{x} = 0$, where

$$\begin{array}{l} \bar{\mathbf{a}}^\top = [\ \bar{H}_{12}\bar{H}_{31},\ \ \bar{H}_{22}\bar{H}_{31},\ \ \ \bar{H}_{11}\bar{H}_{12},\ \ \ \ \bar{H}_{21}\bar{H}_{22},\ \ \ 0\ \ ], \\ \bar{\mathbf{b}}^\top = [\ 2\bar{H}_{11}\bar{H}_{31}, 2\bar{H}_{21}\bar{H}_{31}, \bar{H}_{11}^2 - \bar{H}_{12}^2, \bar{H}_{21}^2 - \bar{H}_{22}^2, \bar{H}_{31}^2\ ]. \end{array} \tag{9}$$

This step can be seen as a first step of Gaussian elimination in system (2) but there is a crucial difference if we are concerned with the error propagation when mapping the elements of $\bar{\mathbf{h}}$ (resp. $\mathbf{h}$) to $\bar{\mathbf{a}}$ and $\bar{\mathbf{b}}$ (resp. $\mathbf{a}$ and $\mathbf{b}$). The algebraic elimination of ω_{33}, as we did previously in [2], yielded coefficients of degree 3 with respect to the elements of $\mathbf{h}$. Here, using the 'compatible' substitution $\mathbf{h} \leftarrow \bar{\mathbf{h}}$, providing that the estimation of the homography matrix $\bar{\mathbf{H}}$ exactly satisfies the constraint $\bar{H}_{32} = 0$, there is no change in the degree of coefficients. This remark seems important to us regarding the behavior of the minimization algorithm.

This step enables us to connect the plane-base calibration problem to the following Poncelet's theorem.

3.2 Poncelet's Theorem

The geometric properties deduced from two planar figures in perspective correspondence and, in particular, about the positions of the centres of projection, are known for a long time, notably thanks to the works of J.V. Poncelet in the middle of the XIX^e century. Within the computer vision community, it is well-known that the pose problem, from a single uncalibrated view of a planar figure, has an infinite number of solutions. Yet, the following Poncelet's theorem[3] [10] tells us that this indetermination has an interesting geometrical interpretation.

Theorem 1. *When a planar figure is the central projection of another planar figure, these figures remain in perspective correspondence when one rotates the plane of the first around its intersection with the plane of the second ; the centre of projection then lies on a circle, in a plane perpendicular to this intersection. As a result, if one projects this circle orthogonally onto the image plane, one obtains a line segment that is the locus of the principal point.*

The Centre Circle and Centre Line. Poncelet's theorem Th. 1 is best explained by referring to Fig. 1. Basically it is said that, given the image of a planar figure, there exists an infinity of 'feasible' world planes on which the planar figure might lie, associated with an infinity of centres of projection. The set of world planes is a pencil whose axis is the intersection line between the image plane and the 'true' world plane. The locus of centres of projection is a circle, called *Centre Circle*, perpendicular to this intersection. The orthogonal projection of the Centre Circle onto the image plane is a line segment, called

[3] We take the liberty to slightly paraphrase the original theorem.

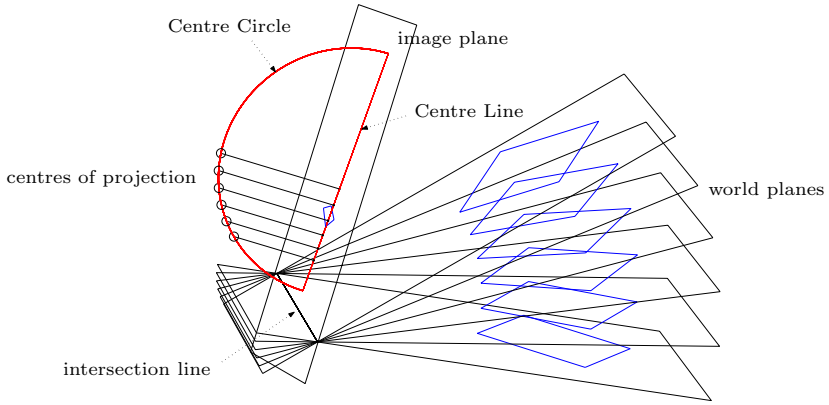

Fig. 1. Illustration of the Poncelet's theorem given as Th. 1.

Centre Line. As the Centre Circle is the camera centre locus in space, the Centre Line is the principal point locus in the image plane.

Poncelet demonstrated Th. 1 in a purely geometrical way. We demonstrated it analytically but, due to space limitation, we only give the proof to the following property ; it will give the reader an idea how to proceed.

The Centre Plane. Denote by L_{Π} the intersection line between the image plane and a world plane Π. Let us call *Centre Plane* of a camera the plane $\mathcal{P}$, passing through the camera centre, whose normal vector is parallel to the line L_{Π} (*i.e.* the Centre Plane contains the Centre Circle).

Property 1 (Centre Plane). If two cameras, with calibration matrices $\mathbf{A}$ and $\mathbf{A}'$ satisfying $\tau = \tau'$, yield exactly the same image of a planar figure, then the centre of the second camera necessarily lies in the Centre Plane $\mathcal{P}$ of the first.

Proof. Let $(\mathbf{R}, \mathbf{t})$ represent the position and orientation of the second camera with respect to the first. It suffices to show that $\mathbf{R}$ is a rotation whose axis is perpendicular to $\mathcal{P}$ and the translation vector $\mathbf{t}$ is parallel to $\mathcal{P}$. If two images are identical, then the inter-image homography matrix $\mathbf{H}_{\Pi}$ induced by Π is the identity transformation, up to a scale factor $\lambda \neq 0$. Let $(\mathbf{n}, d)$ be the representation of world plane Π with respect to the first camera. Suppose that $n_1^2 + n_2^2 > 0$ which means that Π is not parallel to the image plane. From the usual decomposition of $\mathbf{H}_{\Pi}$ [1, § 7.5, p.290], we get

$$\lambda \mathbf{A}'^{-1}\mathbf{A} - (\mathbf{R} + \frac{1}{d}\mathbf{t}\mathbf{n}^{\top}) = \mathbf{0}. \tag{10}$$

It may be seen that $\mathbf{r} = [n_2, -n_1, 0]^{\top}$ is a vector normal to $\mathcal{P}$, *i.e.* parallel to the line L_{Π}, intersecting the first image plane and Π. Also, it is easy to verify that the equality $\mathbf{A}'^{-1}\mathbf{A}\mathbf{r} = \mu\mathbf{r}$ holds, providing that $\tau = \tau'$, where $\mu = \frac{f}{f'} \neq 0$. By right-multiplying both sides of equation (10) by $\mathbf{r}$, we get the equality $(\mathbf{R} - \lambda\mu\mathbf{I})\mathbf{r} = \mathbf{0}$. From this, we infer that $\lambda\mu = 1$ since the unique real eigenvalue of a rotation matrix is 1. axis is perpendicular to $\mathcal{P}$. Now, left-multiply both sides of equation (10) by $\mathbf{r}^{\top}$, then the first two equalities of the resulting equation yield $n_1\mathbf{r}^{\top}\mathbf{t} = 0$

and $n_2\mathbf{r}^\top\mathbf{t} = 0$. Since n_1, n_2 can not be both zero, it follows that $\mathbf{r}^\top\mathbf{t} = 0$, which means that $\mathbf{t}$ is parallel to $\mathcal{P}$.

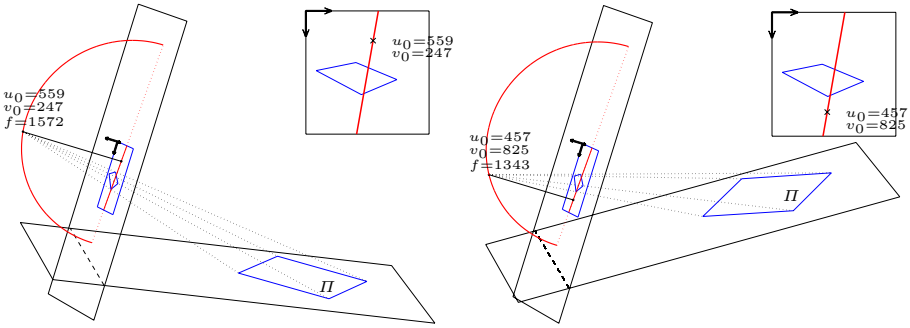

Fig. 2. From one single image with squared pixels (*i.e.* pixel aspect ratio $\tau = 1$), the plane-based calibration problem admits a one-parameter set of solutions. According to Poncelet's theorem (Th. 1), this parameter basically corresponds to the abscissa of the camera centre on the Centre Circle or, equivalently, of the principal point on the Centre Line. As a result, each solution completely determines 'feasible' internal parameters u_0, v_0, f as well as one 'feasible' angle between the image and 3D planes. As an example, two solutions are shown graphically (taken from an animation available at the `URL` given in [3]).

This property will be used in the first step of our 'Centre Circle-based' algorithm. The question now immediately occurs how to relate Poncelet's theorem Th. 1 to the planed-based calibration problem.

3.3 Link Between Th. 1 and Planed-Based Calibration

From one single view of a planar figure, Th. 1 tells us that the set of 'feasible' camera centres defines a circle in the Centre Plane $\mathcal{P}$, *i.e.* the Centre Circle. Now, let us attach a 'τ-corrected' 3D coordinate system to the image, such as the camera centre has Euclidean coordinates $(\tilde{u}_0 = u_0, \tilde{v}_0 = \frac{1}{\tau}v_0, \tilde{w}_0 = -f)$ and the principal point has Euclidean coordinates $(\tilde{u}_0, \tilde{v}_0, 0)$; we call it the *voxel coordinate system.* Each abscissa on the Centre Circle gives one solution $(\tilde{u}_0^*, \tilde{v}_0^*, \tilde{w}_0^*)$, which determines the angle between the image plane and $\mathit{\Pi}$, as is shown in Fig. 2. As mentioned earlier, the orthogonal projection of the Centre Circle onto the image plane (*i.e.* the Centre Line) is the principal point locus in the image plane. Hence, each abscissa on this segment determines one solution $(\tilde{u}_0^*, \tilde{v}_0^*)$ for the principal point.

The Centre Circle can be represented as the intersection between a sphere $\mathcal{S}$ (called *Centre Sphere*) and the Centre Plane $\mathcal{P}$, in the form of the two following equations

$$(\tilde{u} - \tilde{u}_\mathcal{S})^2 + (\tilde{v} - \tilde{v}_\mathcal{S})^2 + (\tilde{w} - \tilde{w}_\mathcal{S})^2 - \rho_\mathcal{S}^2 = 0. \tag{11}$$

$$\eta_1(\tilde{u} - \tilde{u}_\mathcal{P}) + \eta_2(\tilde{v} - \tilde{v}_\mathcal{P}) + \eta_3(\tilde{w} - \tilde{w}_\mathcal{P}) = 0, \tag{12}$$

where $(\tilde{u}, \tilde{v}, \tilde{w})$ are Euclidean point coordinates, with respect to the voxel coordinate system. Eq. (11) is the equation of the Centre Sphere $\mathcal{S}$, with centre $(\tilde{u}_\mathcal{S}, \tilde{v}_\mathcal{S}, \tilde{w}_\mathcal{S})$ and radius $\rho_\mathcal{S}$. Eq. (12) is the equation of the Centre Plane $\mathcal{P}$, passing through $(\tilde{u}_\mathcal{P}, \tilde{v}_\mathcal{P}, \tilde{w}_\mathcal{P})$ and whose normal vector is $\boldsymbol{\eta}$.

Next, we show that it suffices to state $\tilde{u}_\mathcal{P} = \tilde{u}_\mathcal{S}, \;\; \tilde{v}_\mathcal{P} = \tilde{v}_\mathcal{S}, \;\; \tilde{w}_\mathcal{P} = \tilde{w}_\mathcal{S} = 0$ and we necessarily have $\eta_3 = 0$. We also show how to map the five elements of $\bar{\mathbf{H}}$, *i.e.* $\bar{H}_{11}, \bar{H}_{12}, \bar{H}_{21}, \bar{H}_{22}, \bar{H}_{31}$, to the five coefficients $\tilde{u}_\mathcal{P}, \tilde{v}_\mathcal{P}, \eta_1, \eta_2, \rho_\mathcal{S}$.

3.4 Parametrization of the Centre Circle

With reference to § 3.1, we state the following propositions[4].

Proposition 1 (Centre Plane constraint). *Equation* $\bar{\mathbf{a}}^\top \mathbf{x} = 0$ *tells us that the camera centre lies on the Centre Plane* $\mathcal{P}$*, whose equation is (12) with respect to the voxel coordinate system, where*

$$\boldsymbol{\eta} = \left[-\bar{H}_{31}\bar{H}_{12}, \; -\frac{1}{\tau}\bar{H}_{31}\bar{H}_{22}, \; 0 \right]^\top \quad ; \quad \tilde{u}_\mathcal{P} = \frac{\bar{H}_{11}}{\bar{H}_{31}}, \; \tilde{v}_\mathcal{P} = \frac{1}{\tau}\frac{\bar{H}_{21}}{\bar{H}_{31}}, \; \tilde{w}_\mathcal{P} = 0.$$

Proposition 2 (Centre Sphere constraint). *Equation* $\bar{\mathbf{b}}^\top \mathbf{x} = 0$ *tells us the camera centre lies on the Centre Sphere* $\mathcal{S}$*, whose equation is (11) with respect to the voxel coordinate system, where*

$$\tilde{u}_\mathcal{S} = \tilde{u}_\mathcal{P}, \; \tilde{v}_\mathcal{S} = \tilde{v}_\mathcal{P}, \; \tilde{w}_\mathcal{S} = \tilde{w}_\mathcal{P} \quad ; \quad \rho_\mathcal{S} = \frac{\|\boldsymbol{\eta}\|}{\bar{H}_{31}^2} = \frac{\sqrt{\bar{H}_{12}^2 + \tau^{-2}\bar{H}_{22}^2}}{|\bar{H}_{31}|}. \tag{13}$$

It is worthy of note that propositions 1 and 2 are valid, providing that $\bar{H}_{31} \neq 0$ (the case where $\bar{H}_{12}^2 + \bar{H}_{22}^2 = 0$ is impossible) [5]. In fact, $\bar{H}_{31} = 0$ holds if the image plane and Π are parallel, *i.e.* the corresponding intersection line is the line at infinity. Indeed, from the decomposition

$$\bar{\mathbf{H}}_{(:,1:2)} \sim \mathbf{A}\bar{\mathbf{R}} \begin{bmatrix} 1 & 0 \\ 0 & 1 \\ 0 & 0 \end{bmatrix} = \begin{bmatrix} f\bar{R}_{11} + u_0\bar{R}_{31} & f\bar{R}_{12} \\ -\tau f\bar{R}_{21} + v_0\bar{R}_{31} & -\tau f\bar{R}_{22} \\ \bar{R}_{31} & 0 \end{bmatrix} \quad ; \quad \bar{R}_{32} = 0,$$

one can deduce that $\bar{R}_{31} = |\sin\theta|$, where θ is the angle between the image plane and the world plane Π. As a result, we can make two remarks:

- The centre of the sphere lies on the Centre Line, since it lies on both the image plane (*i.e.* $\tilde{w}_\mathcal{S} = 0$) and the Centre Plane (*i.e.* $\tilde{u}_\mathcal{S} = \tilde{u}_\mathcal{P}, \tilde{v}_\mathcal{S} = \tilde{v}_\mathcal{P}, \tilde{w}_\mathcal{S} = \tilde{w}_\mathcal{P}$). Hence, the centre of the Centre Circle coincides with the centre of the Centre Sphere. When $\theta = \frac{\pi}{2}$, the centre of the sphere coincides with the principal point ; when θ decreases, the centre of the sphere moves along the Centre Line (tending towards some point 'at infinity', if θ tends towards 0) ;
- When $\tau = 1$, we have $\rho_\mathcal{S} = \frac{f}{|\sin\theta|}$, with $\lim_{\theta \to 0}(\rho_\mathcal{S}) = +\infty$.

[4] The proofs are omitted.

[5] $\mathcal{S}$ is a real sphere, providing that $\Delta = 4\tau^4(\bar{H}_{31}\bar{H}_{12})^2 + 4\tau^2(\bar{H}_{22}\bar{H}_{31})^2 > 0$ holds.

Our Euclidean framework yields insights into the constraints related to plane-based calibration, as shown in Fig. 3. For a most general framework, Euclidean equations (11) and (12) would have been stated as projective ones, but the geometrical interpretation would be obscured.

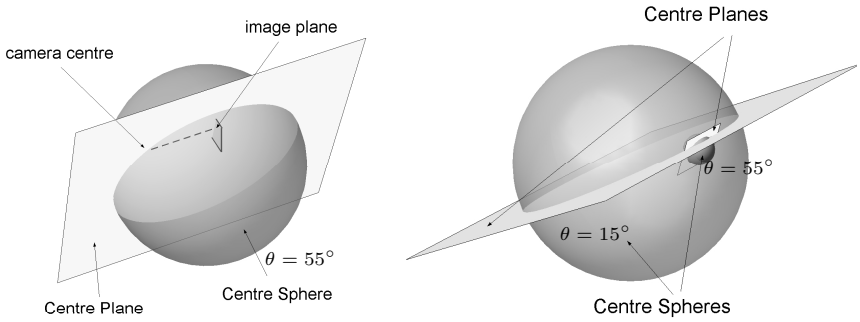

Fig. 3. On the left, the Centre Cercle of a camera is the intersection of the Centre Plane and the Centre Sphere. The Centre Sphere radius depends on the angle θ between the image and the world planes (not drawn). On the right, the spheres of two cameras with same focal length: the largest radius corresponds to $\theta = 15°$, the smallest to $\theta = 55°$.

3.5 The Normalized 'Centre Plane-first' Approach

In the first place, we make it clear that both the Centre Plane and Centre Sphere equations, respectively Eq. (11) and Eq. (12), are linear with respect to the elements of the vector $\mathbf{x}$ that encodes the internal parameters of the camera, as defined in 2.2.A or 2.2.B. However, there is an important difference: the Centre Plane equation is irrespective of the focal length. We now give the following Euclidean properties related to the Centre Plane and Centre Sphere equations.

Let us represent the Euclidean coordinates of any 3D point c, with respect to the voxel coordinate system, by the vector $\mathbf{c} = [\tilde{u}, \tilde{v}, \tilde{w}]^\top$.

1. In Eq. (12), the vector $\boldsymbol{\eta}$ is normal to Centre Plane. If we normalize $\boldsymbol{\eta}$ such as $\|\boldsymbol{\eta}\| = 1$, then it can readily be seen that Eq. (12) represents the distance from the point c to the Centre Plane.
2. Let $\mathsf{c}_\mathcal{S}$ be the centre of the Centre Sphere. On the one hand, we point out that the Eq. (11) represents the power of the point c with respect to the Centre Sphere $\mathcal{S}$. This quantity is indeed defined by $\text{pow}(\mathsf{c}, \mathcal{S}) = \|\mathbf{p} - \mathbf{p}_\mathcal{S}\|^2 - \rho_\mathcal{S}^2$, where $\rho_\mathcal{S}$ is the radius of $\mathcal{S}$, which is invariant under Euclidean transformations. On the other hand, since the radius $\rho_\mathcal{S}$ depends on the focal length and θ (*i.e.* the angle between the image plane and the world plane) according to § 3.4, it is not very meaningful to minimize $\text{pow}(\mathsf{c}, \mathcal{S})$, except if the focal length and θ remain constant during the acquisition. Alternatively, we might approximate the distance from a point c to the sphere $\mathcal{S}$ by the distance from this point to its polar plane with respect to the sphere. Intuitively, this normalization might apply when the distance from c to $\mathcal{S}$ is very small with regard to the radius $\rho_\mathcal{S}$ of $\mathcal{S}$.

The fact that the Centre Plane equation is irrespective of the focal length (which 'unifies' problems 2.2.A or 2.2.B.) plus the difficulty to give a meaning to the Euclidean normalization of Eq. (11), with regard to the minimization criterion, guide us in selecting a two-step algorithm that estimates the internal parameters u_0, v_0, τ alone, irrespective of the focal length f. In accordance with the remark 1, this can be achieved by minimizing Euclidean distances. This 'Centre Plane-first' approach enables us to propose a two-step algorithm: at first, the aspect ratio and the principal point are estimated by minimizing distances to Centre Planes, using the Euclidean normalization of Eq. (12), then each focal length is directly computed from the 'pre-calibrated' views. It can be of interest for plane-based calibration methods that require an off-line pre-calibration step, like in [9]. Our method offers a real strong point: the required amount of flops is now in $\mathcal{O}(m)$, where m is the number of images with different focal lengths, instead of $\mathcal{O}(m^3)$ in the existing ones. The detailed algorithm, also called Centre Line-based algorithm, can be found in a previous paper [2].

3.6 A Two-Step Algorithm for Plane-Based Calibration

Recovering the Internal Parameters. Let the three unknown constant parameters be encoded into the vector $\mathbf{x}$ defined as

$$\mathbf{x} = [\ -u_0\ \ , -\frac{1}{\tau^2} v_0\ \ , \frac{1}{\tau^2}\ ]^\top.$$

Given n homography matrices, let $\bar{\mathbf{F}}$ be the normalized $n \times 4$ matrix obtained by stacking the normalized row vectors $[\bar{a}_1, \bar{a}_2, \bar{a}_4, \bar{a}_3]/(\bar{a}_1^2 + \bar{a}_2^2)^{1/2}$, where $\bar{a}_i$ is defined in (9). According to § 3.5, we can define a left-hand equilibration (diagonal) matrix $\mathbf{W}_L$ such as the least-squares solution satisfies [6]

$$\hat{\mathbf{x}} = \arg\min_{\mathbf{x}} \| \mathbf{W}_L \bar{\mathbf{F}} \left[\mathbf{x}^\top, 1\right]^\top \|^2 \approx \arg\min_{\mathbf{x}} \left(\sum_{j=1}^{n} \mathrm{dist}^2(\mathsf{c}_0, \mathcal{P}^{(j)}) \right),$$

where $\mathrm{dist}(\mathsf{c}_0, \mathcal{P}^{(j)})$ is the Euclidean distance from the camera centre c_0 to the jth Centre Plane $\mathcal{P}^{(j)}$, with respect to the voxel coordinate system.

Recovering the Focal Lengths. This step is detailed in [2].

3.7 Experiments

Simulations. We found out that the Centre Circle algorithm yields the most convincing results when the focal length varies. To illustrate it, we tested it on simulated data, by carrying out comparison tests with the Sturm & Maybank's algorithm described in [11]. Simulations have been achieved using a set of 10 images, with a 512×512 resolution, taken from different positions and orientations of the camera. The camera has constant internal parameters $u_0 = 255, v_0 = 255, \tau = 1$ and a varying focal length f. The calibration object was a $30cm \times 30cm$ planar grid, with 10×10 points. The camera was at a range

[6] We omit the right-hand equilibration for simplicity.

about $2m$ from the observed grid. We chose random values for f and for the angle θ between the image plane and the plane containing the grid, from a uniform distribution on different intervals. Additive Gaussian noise have been added to the projected points, with zero mean and standard deviation $\sigma \in [0.5; 2]$ pixels. The world-to-image homography matrices have been estimated, using the normalized Direct Linear Transformation (DLT) algorithm [4]. As for calibration results, we computed absolute errors (in pixels) for u_0, v_0, relative errors for τ and the 10 focal lengths (in percent). We also counted the rate of computation failures for f, *i.e.* when it could not be recovered. We conducted two tests. Each result presented in Fig. 3.7 was the mean of 1000 independent trials.

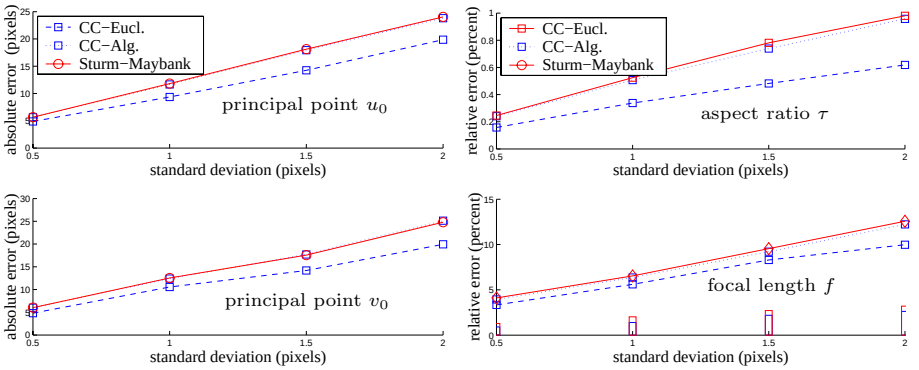

Fig. 4. Calibration results in general configurations: the angle between the image and world planes varies within $]0°, 90°[$ and the focal length varies within $[1000, 2000]$. The best results are obtained using Centre Circle-based (Euclidean) distances.

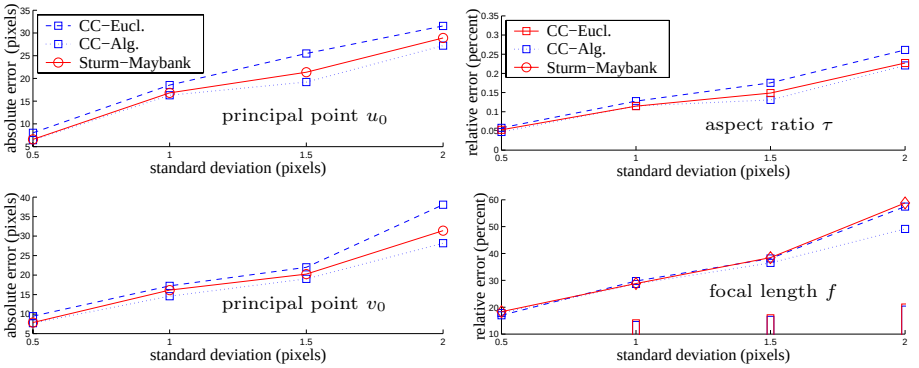

Fig. 5. Calibration results in presence of singular configurations: the angle varies within $]1°, 10°[$. The best results are obtained using Centre Circle-based (algebraic) distances. We currently investigate how to automatically select the adequate distance.

Test 1. For each trial, the 10 focal lengths took different values within interval $[1000, 2000]$ (in pixels), while θ varied within $]0°, 90°[$. In Fig. 3.7, the solid lines show the errors associated with the Sturm & Maybank's algorithm. The dotted

(resp. dashed) lines show the errors associated with the Centre Circle algorithm without (resp. with) Euclidean normalization of equations. As a result, we can point out that the Euclidean normalization of equations improved the accuracy of the results. The gain in accuracy is around 2σ for u_0, v_0 and $\sigma\%$ for f. The rate of computation failures for f is around 3% for $\sigma = 2$.

Test 2. The second test differed from the first, owing to the fact that θ varied within interval $]0°, 10°[$, in order to test how the Centre Circle algorithm behaved in presence of singular configurations, *i.e.* when the planar grid was nearly parallel to the image plane. Actually, even in this case, the Centre Circle algorithm yielded the best results, although it was very close in precision to Sturm & Maybank's results. Nevertheless, as it may be seen in Fig. 3.7, it is not recommended to use the Euclidean normalization in this case. The problem with Euclidean normalizations here is due to the division of the Centre Plane coefficients by the norm of a vector which is collinear to the line intersecting the image and world planes. When the angle between these planes tends towards 0, the vector tends towards the null vector. Without Euclidean normalization, the Centre Circle-based algorithm still yields the best results. The gain in accuracy is around σ for u_0, v_0. It is worthy of note that, like in Test 1, the Centre Circle algorithm exhibits the smallest rate of computation failures (around 20% for $\sigma = 2$) as well as the smallest errors on f.

Real Images As seen in Fig. 6, we checked the Centre Circle-based algorithm with 6 real images of a calibration grid taken at a distance of about $40cm$ from different positions. Images are taken by a NIKON COOLPIX 800 in a 1600×1200 *jpeg* format with the maximal setting of zoom. We know that the bigger zoom is used, the less distortion is present in the images. There has been small variations of the focal length during the auto-focusing. The recovered internal parameters are $u_0 = 810.14$, $v_0 = 558.32$, $\tau = 1.0026$, $f^{(1)} = 3472.95$, $f^{(2)} = 3507.95$, $f^{(3)} = 3656.54$, $f^{(4)} = 3479.40$, $f^{(5)} = 3402.76$, $f^{(6)} = 3465.67$. The residual error vector, whose elements are orthogonal distances from the estimated principal point to the Centre Lines (*i.e.* the lines intersecting the Centre Planes and the image plane), has mean 5.5 pixels with standard deviation 5.8.

4 Conclusion

The usual formulation of plane-based calibration of a camera is based on properties of basis vector with respect to the observed plane. For constant internal parameters [14][7] (or varying internal parameters [11]), a solution can be obtained by minimizing an algebraic cost function using a direct method.

Our contribution is to put the problem into a more intuitive geometric framework, in accordance to a Poncelet's theorem, which enables us to give an Euclidean interpretation to the plane-based calibration equations. The proposed algorithm is carried out through a two-step process: at first, the aspect ratio and the principal point are estimated, after which each focal length is directly computed. This approach is said to be 'Centre Plane-first' since the problem is first that of minimizing distances from the camera centre to a set of Centre

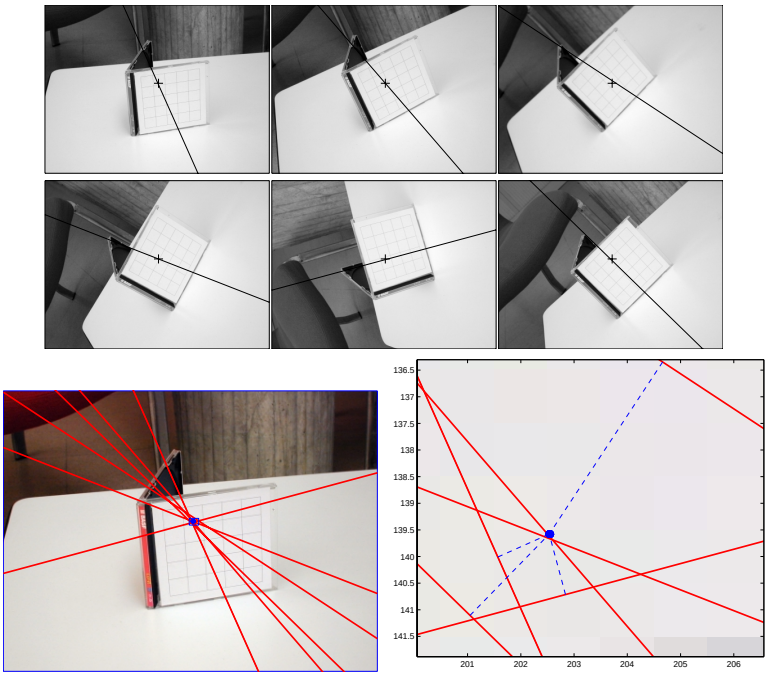

Fig. 6. At top, the plane-based calibration from 6 views of a planar grid sticked on a CD jewel case, taken by a camera with different focal lengths. The estimated principal point is plotted with a cross and the different Centre Lines (*i.e.* the lines intersecting the Centre Planes and the image plane) are displayed in each view. In the left-hand image at bottom, the 'pencil' of Centre Lines is plotted with respect to the first image frame. In the right-hand image at bottom, by zooming the window near the principal point with a factor 100, the plane-based calibration problem is that of minimizing orthogonal distances from the camera centres to the different Centre Planes or, equivalently, from the principal point to the different Centre Lines.

Planes (or equivalently from the principal point to a set of Centre Lines). It offers a real advantage: the required amount of flops, for recovering all internal parameters, is in $\mathcal{O}(n)$ while it was in $\mathcal{O}(n^3)$ in the existing one. Our algorithms yield the most accurate results, especially when the focal length varies.

One can argue that a better accuracy is generally obtained when all parameters are estimated simultaneously. However, the estimation of parameter matrix $\boldsymbol{\omega}$ through the linearization of basic equations (2) must be discussed. All the existing direct solutions to the plane-based calibration problem are obtained through the linearization of a nonlinear errors-in-variables model [5]. Indeed, the mapping of $\mathbf{H}$ to matrix $\left[\,\mathbf{a} \mid \mathbf{b}\,\right]^\top$ is nonlinear in (6), which means that we actually solve $\left[\,\mathbf{a}(\mathbf{H}) \mid \mathbf{b}(\mathbf{H})\,\right]^\top \mathbf{x} = \mathbf{0}$, using a total least squares (TLS) approach [5]. It theorically requires heteroscedastic regression [6], *i.e.* to take in account that errors on vectors $\mathbf{a}$, $\mathbf{b}$ can have nonzero mean and different covariance matrices.

From a statistical point of view, it can be shown [6] that a TLS solution can introduce a bias, in particular when mapping $\mathbf{H}$ to the vector $\mathbf{b}$. This stems from the fact that the elements of $\mathbf{b}$ have squared terms. This drawback notably appears under the assumption that the errors $\Delta\mathbf{H}$ in $\mathbf{H}$ are independently distributed with zero mean, as soon as the covariance matrix $\boldsymbol{\Sigma}_{\Delta\mathbf{H}}$ is diagonal with different variances. The good accuracy of the incremental results, with our 'Centre Plane-first' algorithm, can be explained in part by the fact that the equation associated with $\mathbf{b}$ (*i.e.* with the Centre Sphere) is not used in its first step.

References

1. O. Faugeras. Three-Dimensional Computer Vision: a Geometric Viewpoint. The MIT Press, Cambridge, Massachusetts, USA. 1993.
2. P. Gurdjos and R. Payrissat. Plane-based Calibration of a Camera with Varying Focal Length: the Centre Line Constraint. In Proc. of the 12th British Machine Vision Conference (BMVC'01), Manchester, UK, pp. 623-632. September 2001.
3. `http://www.irit.fr/~Pierre.Gurdjos/ECCV2002/`
4. R. Hartley and A. Zisserman. Multiple View Geometry in Computer Vision. Cambridge University Press, Cambridge, UK. 2000.
5. S. Van Huffel and J. Vandewalle. The total least squares problem: computational aspects and analysis. Frontiers in Applied Mathematics series, vol. 9, SIAM, Philadelphia, Pennsylvania, USA. 1991.
6. Y. Leedan and P. Meer. Heteroscedastic Regression in Computer Vision: Problems with Bilinear Constraint. International Journal of Computer Vision (IJCV), vol. 37, no. 2, p. 127-150. 2000.
7. D. Liebowitz and A. Zisserman. Combining Scene and Auto-Calibration Constraints. In Proc. of the 7th International Conference on Computer Vision (ICCV'99), Kerkyra, Greece. September 1999.
8. E. Malis and R. Cipolla. Self-Calibration of Zooming Cameras Observing an Unknown Planar Structure. In Proc. of the 15th International Conference on Pattern Recognition (ICPR'00), vol. 1, pp. 85-88, Barcelona, Spain. September 2000.
9. C. Matsunaga and K. Kanatani. Calibration of a Moving Camera Using a Planar Pattern: Optimal Computation, Reliability Evaluation, and Stabilization by Model Selection. In Proc. of the 6th European Conference on Computer Vision (ECCV'00), Dublin, Ireland. July 2000.
10. J.-V. Poncelet. Applications d'Analyse et de Géometrie - Traité des Propriétés Projectives des Figures. Tome I. Imprimerie de Mallet-Bachelier, Paris. 1862.
11. P. Sturm and S. Maybank. On Plane-Based Camera Calibration: a General Algorithm, Singularities, Applications. In Proc. of the Computer Vision and Pattern Recognition Conference (CVPR'99), Fort Collins, Colorado, USA, pp. 432-437. June 1999.
12. P. Sturm. Algorithms for Plane-Based Pose Estimation. In Proc. of the Computer Vision and Pattern Recognition Conference (CVPR'00), Hilton Head, USA, pp. 1010-1017. June 2000.
13. B. Triggs. Autocalibration from Planar Scenes. In Proc. of the 5th European Conference on Computer Vision (ECCV'98), pp. 89-105, Freiburg, Germany. June 1998.
14. Z. Zhang. A Flexible New Technique for Camera Calibration. IEEE Transactions on Pattern Analysis and Machine Intelligence (PAMI), vol. 22, no. 11, pp. 1330-1344. 2000.